1-1-2005

A generalized algorithm for the generation of correlated Rayleigh fading envelopes in wireless channels

Le Chung Tran
University of Wollongong, lctran@uow.edu.au

Tadeusz A. Wysocki
University of Wollongong, wysocki@uow.edu.au

Alfred Mertins
University of Oldenburg, mertins@uow.edu.au

Jennifer R. Seberry
University of Wollongong, jennie@uow.edu.au

A generalized algorithm for the generation of correlated Rayleigh fading envelopes in wireless channels

Abstract

Although generation of correlated Rayleigh fading envelopes has been intensively considered in the literature, all conventional methods have their own shortcomings, which seriously impede their applicability. In this paper, a very general, straightforward algorithm for the generation of an *arbitrary* number of Rayleigh envelopes with any desired, equal or unequal power, in wireless channels either *with* or *without* Doppler frequency shifts, is proposed. The proposed algorithm can be applied to the case of *spatial correlation*, such as with multiple antennas in Multiple Input Multiple Output (MIMO) systems, or *spectral correlation* between the random processes like in Orthogonal Frequency Division Multiplexing (OFDM) systems. It can also be used for generating correlated Rayleigh fading envelopes in either *discrete-time instants* or a *real-time scenario*. Besides being *more generalized*, our proposed algorithm is *more precise*, while overcoming all shortcomings of the conventional methods.

Keywords

Generalized, Algorithm, for, Generation, Correlated, Rayleigh, Fading, Envelopes, Wireless, Channels

Disciplines

Physical Sciences and Mathematics

Publication Details

Tran, L., Wysocki, T. A., Seberry, J. R. & Mertins, A. (2005). A generalized algorithm for the generation of correlated Rayleigh fading envelopes in wireless channels. EURASIP Journal on Wireless Communications and Networking, 801-815.

A Generalized Algorithm for the Generation of Correlated Rayleigh Fading Envelopes in Wireless Channels

Le Chung Tran, *Member, IEEE,* Tadeusz A. Wysocki, *Senior Member, IEEE*, Alfred Mertins, *Senior Member, IEEE,* and Jennifer Seberry, *Senior Member, IEEE*

Abstract

Although generation of correlated Rayleigh fading envelopes has been intensively considered in the literature, all conventional methods have their own shortcomings, which seriously impede their applicability. In this paper, a very general, straightforward algorithm for the generation of an *arbitrary* number of Rayleigh envelopes with *any desired, equal or unequal* power, in wireless channels either *with* or *without* Doppler frequency shifts, is proposed. The proposed algorithm can be applied to the case of *spatial correlation*, such as with multiple antennas in Multiple Input Multiple Output (MIMO) systems, or *spectral correlation* between the random processes like in Orthogonal Frequency Division Multiplexing (OFDM) systems. It can also be used for generating correlated Rayleigh fading envelopes in either *discrete-time instants* or a *real-time scenario*. Besides being *more generalized*, our proposed algorithm is *more precise*, while overcoming all shortcomings of the conventional methods.

Index Terms

Correlated Rayleigh fading envelopes, antenna arrays, OFDM, MIMO, Doppler frequency shift.

I. Introduction

In Orthogonal Frequency Division Multiplexing (OFDM) systems, the fading affecting carriers may have cross-correlation due to the small coherence bandwidth of the channel, or due to the inadequate frequency separation between the carriers. In addition, in Multiple Input Multiple Output (MIMO) systems where multiple antennas are used to transmit and/or receive signals, the fading affecting these antennas

Some results included in this paper were presented during the 5th IEEE International Workshop on Algorithms for Wireless, Mobile, Ad Hoc and Sensor Networks (IEEE WMAN 05), Apr. 2005 and during the IEEE International Symposium on a World of Wireless, Mobile and Multimedia Networks (IEEE WOWMOM), June 2005.

may also experience cross-correlation due to the inadequate separation between the antennas. Therefore, a generalized, straightforward and, certainly, correct algorithm to generate correlated Rayleigh fading envelopes is required for the researchers wishing to analyze theoretically and simulate the performance of systems.

Because of that, generation of correlated Rayleigh fading envelopes has been intensively mentioned in the literature, such as [1] – [13]. However, besides not being adequately generalized to be able to apply to various scenarios, all conventional methods have their own shortcomings which seriously limit their applicability or even cause failures in generating the desired Rayleigh fading envelopes.

In this paper, we modify existing methods and propose a generalized algorithm for generating correlated Rayleigh fading envelopes. Our modifications are *simple*, but *important* and also very *efficient*. The proposed algorithm thus incorporates the advantages of the existing methods, while overcoming all of their shortcomings. Furthermore, besides being *more generalized*, the proposed algorithm is *more accurate*, while providing *more useful features* than the conventional methods.

The paper is organized as follows. In Section II, a summary of the shortcomings of conventional methods for generating correlated Rayleigh fading envelopes is derived. In Section III-A and Section III-B, we shortly review the discussions on the correlation property between the transmitted signals as functions of time delay and frequency separation, such as in OFDM systems, and as functions of spatial separation between transmission antennas, such as in MIMO systems, respectively. In Section IV, we propose a very general, straightforward algorithm to generate correlated Rayleigh fading envelopes. Section V derives an algorithm to generate correlated Rayleigh fading envelopes in a real-time scenario. Simulation results are presented in Section VI. The paper is concluded by Section VII.

II. Shortcomings of Conventional Methods and Aims of the Proposed Algorithm

We first analyze the shortcomings of some conventional methods for the generation of correlated Rayleigh fading envelopes.

In [2], the authors derived fading correlation properties in antenna arrays and, then, briefly mentioned the algorithm to generate complex Gaussian random variables (with Rayleigh envelopes) corresponding to a desired correlation coefficient matrix. This algorithm was proposed for generating *equal power* Rayleigh envelopes only, rather than *arbitrary* (*equal or unequal*) power Rayleigh envelopes.

In the papers [7] and [8], the authors proposed different methods for generating only N*=2 equal power* correlated Rayleigh envelopes. In [4], the authors generalized the method of [8] for $N \geq 2$. However, in this method, Cholesky decomposition [14] is used, and consequently, the covariance matrix must be

positive definite, which is not always realistic. An example, where the covariance matrix is *not* positive definite, is derived later in Example 4.1 of Section IV-A of this paper.

These methods were then more generalized in [9], where one can generate *any number* of Rayleigh envelopes corresponding to a desired covariance matrix and with *any power*, i.e., even with *unequal* power. However, again, the covariance matrix *must be positive definite* in order for Cholesky decomposition to be performable. In addition, the authors in [9] forced the covariances of the complex Gaussian random variables (with Rayleigh fading envelopes) to be *real* (see Eq. (8) in [9]). This limitation *prohibits* the use of their method in various cases because, in fact, the covariances of the complex Gaussian random variables are more likely to be complex.

In [13], the authors proposed a method for generating *any number* of Rayleigh envelopes with *equal power* only. Although the method of [13] works well in various cases, it *fails* to perform Cholesky decomposition for some complex covariance matrices in MatLab due to the roundoff errors of Matlab [1]. This shortcoming is overcome by some modifications mentioned later in our proposed algorithm.

More importantly, the method proposed in [13] *fails* to generate Rayleigh fading envelopes corresponding to a desired covariance matrix in a real-time scenario *where Doppler frequency shifts are considered*. This is because passing Gaussian random variables with variances assumed to be equal to one (for simplicity of explanation) through a Doppler filter changes remarkably the variances of those variables. The variances of the variables at the outputs of Doppler filters are *not* equal to one any more, but depend on the variance of the variables at the inputs of the filters as well as the characteristics of those filters. The authors in [13] did not realize this variance-changing effect caused by Doppler filters. We will return to this issue later in this paper.

For the aforementioned reasons, a *more generalized* algorithm is required to generate *any number* of Rayleigh fading envelopes with *any power* (*equal or unequal* power) corresponding to *any desired* covariance matrix. The algorithm should be applicable to both *discrete time instant* scenario and *real-time* scenario. The algorithm is also expected to overcome roundoff errors which may cause the interruption

[1]It has been well known that Cholesky decomposition may not work for the matrix having eigenvalues being equal or close to zeros. We consider the following covariance matrix $\mathcal{K}$, for instance:

$$\mathcal{K} = \begin{bmatrix} 1.04361 & 0.7596 - 0.3840i & 0.6082 - 0.4427i & 0.4085 - 0.8547i \\ 0.7596 + 0.3840i & 1.04361 & 0.7780 - 0.3654i & 0.6082 - 0.4427i \\ 0.6082 + 0.4427i & 0.7780 + 0.3654i & 1.04361 & 0.7596 - 0.3840i \\ 0.4085 + 0.8547i & 0.6082 + 0.4427i & 0.7596 + 0.3840i & 1.04361 \end{bmatrix}$$

Cholesky decomposition does not work for this covariance matrix although it is positive definite.

of Matlab programs. In addition, the algorithm should work well, regardless of the positive definiteness of the covariance matrices. Furthermore, the algorithm should provide a straightforward method for the generation of complex Gaussian random variables (with Rayleigh envelopes) with correlation properties as functions of *time delay* and *frequency separation* (such as in OFDM systems), or *spatial separation* between transmission antennas (like with multiple antennas in MIMO systems). This paper proposes such an algorithm.

III. Brief Review of Studies on Fading Correlation Characteristics

In this section, we shortly review the discussions on the correlation property between the transmitted signals as functions of time delay and frequency separation, such as in OFDM systems, and as functions of spatial separation between transmission antennas, such as in MIMO systems. These discussions were originally derived in [15] and in [2], respectively.

This review aims at facilitating readers to apply our proposed algorithm in different scenarios (i.e. *spectral correlation*, such as in OFDM systems, or *spatial correlation*, such as in MIMO systems) as well as pointing out the condition for the analyses in [15] and in [2] to be applicable to our proposed algorithm (i.e. these analyses are applicable to our algorithm if the powers (variances) of different random processes are assumed to be the same).

A. Fading Correlation as Functions of Time Delay and Frequency Separation

In [15], Jakes considered the scenario where all complex Gaussian random processes with Rayleigh envelopes have *equal* powers σ^2 and derived the correlation properties between random processes as functions of both time delay and frequency separation, such as in OFDM systems. Let $z_k(t)$ and $z_j(t)$ be the two zero-mean complex Gaussian random processes at time instant t, corresponding to frequencies f_k and f_j, respectively. Denote:

$$\begin{aligned} x_k &\triangleq Re(z_k(t)); \qquad & y_k &\triangleq Im(z_k(t)) \\ x_j &\triangleq Re(z_j(t+\tau_{k,j})); \qquad & y_j &\triangleq Im(z_j(t+\tau_{k,j})) \end{aligned}$$

where $\tau_{k,j}$ is the arrival time delay between two signals and $Re(.)$, $Im(.)$ are the real and imaginary parts of the argument, respectively. By definition, the covariances between the real and imaginary parts of $z_k(t)$ and $z_j(t+\tau_{k,j})$ are:

$$R_{xx_{k,j}} \triangleq E(x_k x_j); \qquad R_{yy_{k,j}} \triangleq E(y_k y_j) \tag{1}$$

$$R_{xy_{k,j}} \triangleq E(x_k y_j); \qquad R_{yx_{k,j}} \triangleq E(y_k x_j) \tag{2}$$

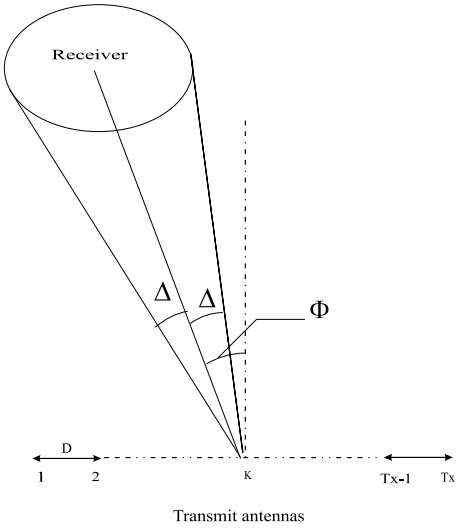

Fig. 1. Model to examine the spatial correlation between transmitter antennas.

Then, those covariances have been derived in [15] (see Eq. (1.5-20)) as:

$$R_{xx_{k,j}} = R_{yy_{k,j}} = \frac{\sigma^2 J_0(2\pi F_m \tau_{k,j})}{2[1+(\Delta\omega_{k,j}\sigma_\tau)^2]} \quad (3)$$

$$R_{xy_{k,j}} = -R_{yx_{k,j}} = -\Delta\omega_{k,j}\sigma_\tau R_{xx_{k,j}} \quad (4)$$

where σ^2 is the variance (power) of the complex Gaussian random processes ($\frac{\sigma^2}{2}$ is the variance per dimension);

J_0 is the first-kind Bessel function of the zeroth-order;

F_m is the maximum Doppler frequency F_m=$\frac{v}{\lambda}$ =$\frac{vf_c}{c}$. In this formula, λ is the wavelength of the carrier, f_c is the carrier frequency, c is the speed of light and v is the mobile speed;

$\Delta\omega_{k,j}$=$2\pi(f_k - f_j)$ is the angular frequency separation between the two complex Gaussian processes with Rayleigh envelopes at frequencies f_k and f_j;

σ_τ is the root-mean-square (rms) delay spread of the wireless channel.

It should be emphasized that, the equalities (3) and (4) hold only when the set of *multi-path channel coefficients*, which were denoted as C_{nm} and derived in Eq. (1.5-1) and (1.5-2) in [15], as well as the *powers* are assumed to be the *same* for different random processes (with different frequencies). Readers may refer to [15] (pp. 46–49) for an explicit exposition.

B. Fading Correlation as Functions of Spatial Separation in Antenna Arrays

The fading correlation properties between wireless channels as functions of antenna spacing in multiple antenna systems have been mentioned in [2]. Fig. 1 presents a typical model of the channel where all

signals from a receiver are assumed to arrive at T_x antennas within $\pm\Delta$ at angle Φ ($|\Phi| \leq \pi$). Let λ be the wavelength, D the distance between the two adjacent transmitter antennas, and $z = 2\pi\frac{D}{\lambda}$. In [2], it is assumed that fading corresponding to different receivers is independent. This is reasonable if receivers are not on top of each other within some wavelengths and they are surrounded by their own scatterers. Consequently, we only need to calculate the correlation properties for a typical receiver. The fading in the channel between a given k^{th} transmitter antenna and the receiver may be considered as a zero-mean, complex Gaussian random variable, which is presented as $b^{(k)} = x^{(k)} + iy^{(k)}$. Denote the covariances between the real parts as well as the imaginary parts themselves of the fading corresponding to the k^{th} and j^{th} transmitter antennas[2] to be $R_{xxk,j}$ and $R_{yy_{k,j}}$, while those terms between the real and imaginary parts of the fading to be $R_{xy_{k,j}}$ and $R_{yx_{k,j}}$. The terms $R_{xxk,j}$, $R_{yy_{k,j}}$, $R_{xy_{k,j}}$ and $R_{yx_{k,j}}$ are similarly defined as (1) and (2). Then, it has been proved that the closed-form expressions of these covariances normalized by the variance per dimension (real and imaginary) are (see Eq. (A. 19) and (A. 20) in [2]):

$$\tilde{R_{xxk,j}} = \tilde{R_{yy_{k,j}}} = J_0(z(k-j)) + 2\sum_{m=1}^{\infty} J_{2m}(z(k-j))cos(2m\Phi)\frac{sin(2m\Delta)}{2m\Delta} \tag{5}$$

$$\tilde{R_{xy_{k,j}}} = -\tilde{R_{yx_{k,j}}} = 2\sum_{m=0}^{\infty}\left[J_{2m+1}(z(k-j))sin[(2m+1)\Phi]\frac{sin[(2m+1)\Delta]}{(2m+1)\Delta}\right] \tag{6}$$

where $\tilde{R}_{k,j} = \frac{2R_{k,j}}{\sigma^2}$. In other words, we have:

$$R_{k,j} = \frac{\sigma^2\tilde{R}_{k,j}}{2} \tag{7}$$

In these equations, J_q is the first-kind Bessel function of the integer order q, and $\sigma^2/2$ is the variance per dimension of the received signal at each transmitter antenna, i.e., it is assumed in [2] that the signals corresponding to different transmitter antennas have *equal* variances σ^2.

Similarly to Section III-A, the equalities (5) and (6) hold only when the set of *multi-path channel coefficients*, which were denoted as g_n and derived in Eq. (A-1) in [2], and the *powers* are assumed to be the *same* for different random processes. Readers may refer to [2] (pp. 1054–1056) for an explicit exposition.

[2]Note that k and j here are antenna indices, while they are frequency indices in Section III-A.

IV. Generalized Algorithm to Generate Correlated, Flat Rayleigh Fading Envelopes

A. Covariance Matrix of Complex Gaussian Random Variables with Rayleigh Fading Envelopes

It is known that Rayleigh fading envelopes can be generated from zero-mean, complex Gaussian random variables. We consider here a column vector $\mathbb{Z}$ of N zero-mean, *complex* Gaussian random variables with variances (or powers) $\sigma_{g_j}^2$, for $j = 1, \ldots, N$. Denote $\mathbb{Z} = (z_1, \ldots, z_N)^T$, where z_j ($j = 1, \ldots, N$) is regarded as:

$$z_j \;=\; r_j e^{i\theta_j} = x_j + iy_j$$

The modulus of z_j is: $r_j = \sqrt{x_j^2 + y_j^2}$. It is assumed that the phases θ_js are independent, identically uniformly distributed random variables. As a result, the real and imaginary parts of each z_j are independent (but z_js are not necessarily independent), i.e., the covariances $E(x_j y_j) = 0$ for $\forall j$ and therefore, r_js are *Rayleigh envelopes*.

Let $\sigma_{g_{xj}}^2$ and $\sigma_{g_{yj}}^2$ be the variances per dimension (real and imaginary), i.e., $\sigma_{g_{xj}}^2 = E(x_j^2)$, $\sigma_{g_{yj}}^2 = E(y_j^2)$. Clearly, $\sigma_{g_j}^2 = \sigma_{g_{xj}}^2 + \sigma_{g_{yj}}^2$. If $\sigma_{g_{xj}}^2$=$\sigma_{g_{yj}}^2$, then $\sigma_{g_{xj}}^2$=$\sigma_{g_{yj}}^2$=$\frac{\sigma_{g_j}^2}{2}$. Note that we consider a very general scenario where the variances (powers) of the real parts are not necessarily equal to those of the imaginary parts. Also, the powers of Rayleigh envelopes denoted as $\sigma_{r_j}^2$ are not necessarily equal to one another. Therefore, the scenario where the variances of the Rayleigh envelopes are equal to one another and the powers of real parts are equal to those of imaginary parts, such as the scenario mentioned in either Section III-A or Section III-B, is considered as a particular case.

For $k \neq j$, we define the covariances $R_{xx_{k,j}}$, $R_{yy_{k,j}}$, $R_{xy_{k,j}}$ and $R_{yx_{k,j}}$ between the real as well as imaginary parts of z_k and z_j, similarly to those mentioned in (1) and (2).

By definition, the covariance matrix $\mathcal{K}$ of $\mathbb{Z}$ is:

$$\mathcal{K} \;=\; E(\mathbb{Z}\mathbb{Z}^H) \stackrel{\Delta}{=} [\mu_{k,j}]_{N\times N} \tag{8}$$

where $(.)^H$ denotes the Hermitian transposition operation and

$$\mu_{k,j} = \begin{cases} \sigma_{g_j}^2 & \text{if } k \equiv j \\ (R_{xx_{k,j}} + R_{yy_{k,j}}) - i(R_{xy_{k,j}} - R_{yx_{k,j}}) & \text{if } k \neq j \end{cases} \tag{9}$$

In reality, the covariance matrix $\mathcal{K}$ is *not* always positive semi-definite. An example where the covariance matrix $\mathcal{K}$ is *not* positive semi-definite is derived as follows.

Example 4.1: We examine an antenna array comprising 3 transmitter antennas. Let D_{kj}, for $k, j = 1, \ldots, 3$, be the distance between the k^{th} antenna and the j^{th} antenna. The distance D_{jk} between j^{th}

antenna and the k^{th} antenna is then $D_{jk} = -D_{kj}$. Specifically, we consider the case:

$$\begin{aligned} D_{21} &= 0.0385\lambda \\ D_{31} &= 0.1789\lambda \\ D_{32} &= 0.1560\lambda \end{aligned}$$

where λ is the wavelength. Clearly, these antennas are *neither* equally spaced, *nor* positioned in a straight line. Instead, they are positioned at the 3 peaks of a triangle.

If the receiver antenna is far enough from the transmitter antennas, we can assume that all signals from the receiver arrive at the transmitter antennas within $\pm\Delta$ at angle Φ (see Fig. 1 for the illustration of these notations). As a result, the analytical results mentioned in Section III-B with small modifications can still be applied to this case. In particular, covariance matrix $\mathcal{K}$ can still be calculated following (5), (6), (7), (8) and (9), provided that, in (5) and (6), the products $z(k-j)$ (or $2\pi D(k-j)/\lambda$) are replaced by $2\pi D_{kj}/\lambda$. This is because, in our considered case, D_{kj} are the actual distances between the k^{th} transmitter antenna and the j^{th} transmitter antenna, for $k, j = 1, \ldots, 3$.

Further, we assume that the variance σ^2 of the received signals at each transmitter antenna in (7) is unit, i.e., $\sigma^2 = 1$. We also assume that $\Phi = 0.1114\pi$ rad and $\Delta = 0.1114\pi$ rad.

In order to examine the performance of the considered system, the Rayleigh fading envelopes are required to be simulated. In turn, the covariance matrix of the complex Gaussian random variables corresponding to these Rayleigh envelopes must be calculated. Based on the aforementioned assumptions, from the theoretically analytical equations (5), (6), (7), and the definition equations (8) and (9), we have the following desired covariance matrix for the considered configuration of transmitter antennas:

$$\mathcal{K} = \begin{bmatrix} 1.0000 & 0.9957 + 0.0811i & 0.9090 + 0.3607i \\ 0.9957 - 0.0811i & 1.0000 & 0.9303 + 0.3180i \\ 0.9090 - 0.3607i & 0.9303 - 0.3180i & 1.0000 \end{bmatrix} \quad (10)$$

Performing eigen decomposition, we have the following eigenvalues -0.0092; 0.0360; and 2.9733. Therefore, $\mathcal{K}$ is *not* positive semi-definite. This also means that $\mathcal{K}$ is *not* positive definite.

It is important to emphasize that, from the mathematical point of view, covariance matrices are *always* positive semi-definite by definition (8), i.e. the eigenvalues of the covariance matrices are *either* zero *or* positive. However, this does not contradict the above example where the covariance matrix $\mathcal{K}$ has a negative eigenvalue. The main reason why the desired covariance matrix $\mathcal{K}$ is not positive semi-definite is due to the approximation and the simplifications of the model mentioned in Fig. 1 in calculating the

covariance values, i.e., due to the preciseness of the equations (5) and (6), compared to the true covariance values. In other words, errors in estimating covariance values may exist in the calculation. Those errors may result in a covariance matrix being not positive semi-definite.

A question that could be raised here is why the covariance matrix of *complex Gaussian random variables* (with Rayleigh fading envelopes), rather than the covariance matrix of *Rayleigh envelopes*, is of particular interest. This is due to the two following reasons.

From the physical point of view, in the covariance matrix of *Rayleigh envelopes*, the correlation properties R_{xx}, R_{yy} of the real components (in-phase components) as well as the imaginary components (quadrature phase components) themselves and the correlation properties R_{xy}, R_{yx} between the real and imaginary components of random variables are *not* directly present (these correlation properties are defined in (1) and (2)). On the contrary, those correlation properties are *clearly* present in the covariance matrix of complex Gaussian random variables with the desired Rayleigh envelopes. In other words, the physical significance of the correlation properties of random variables is *not* present as detailed in the covariance matrix of *Rayleigh envelopes* as in the covariance matrix of complex Gaussian random variables with the desired Rayleigh envelopes.

Further, from the mathematical point of view, it is possible to have one-to-one mapping *from* the cross-correlation coefficients ρ_{gij} (between the i^{th} and j^{th} complex Gaussian random variables) *to* the cross-correlation coefficients ρ_{rij} (between Rayleigh fading envelopes) as follows (see Eq. (1.5-26) in [15]):

$$\rho_{rij} = \frac{(1+|\rho_{gij}|)E_{int}\left(\frac{2\sqrt{|\rho_{gij}|}}{1+|\rho_{gij}|}\right) - \frac{\pi}{2}}{2-\frac{\pi}{2}}$$

where $E_{int}(.)$ is the complete elliptic integral of the second kind. Some good approximations of this relationship between ρ_{rij} and ρ_{gij} are presented in the mapping table II in [7], the look-up Table I and Fig. 1 in [9].

However, the reversed mapping, i.e. the mapping *from* ρ_{rij} *to* ρ_{gij}, is *multivalent*. It means that, for a given ρ_{rij}, we have to somehow determine ρ_{gij} in order to generate Rayleigh fading envelopes and the possible values of ρ_{gij} may be significantly different from each other depending on how ρ_{gij} is determined from ρ_{rij}. It is noted that ρ_{rij} is always real, but ρ_{gij} may be complex.

For the two aforementioned reasons, the covariance matrix of complex Gaussian random variables (with Rayleigh envelopes), as opposed to the covariance matrix of Rayleigh envelopes, is of particular interest in this paper.

B. Forced Positive Semi-definiteness of the Covariance Matrix

First, we need to define the *coloring matrix* $\mathcal{L}$ corresponding to a covariance matrix $\mathcal{K}$. The *coloring matrix* $\mathcal{L}$ is defined to be the $N \times N$ matrix satisfying:

$$\mathcal{L}\mathcal{L}^H = \mathcal{K}$$

It is noted that the coloring matrix is *not* necessarily a lower triangular matrix. Particularly, to determine the coloring matrix $\mathcal{L}$ corresponding to a covariance matrix $\mathcal{K}$, we can use *either* Cholesky decomposition [14] as mentioned in a number of papers, which have been reviewed in Section II of this paper, *or* eigen decomposition which is mentioned in the next section of this paper. The former yields a lower triangular coloring matrix, while the later yields a square coloring matrix.

Unlike Cholesky decomposition, where the covariance matrix $\mathcal{K}$ must be *positive definite*, eigen decomposition requires that $\mathcal{K}$ is at least *positive semi-definite*, i.e. the eigenvalues of $\mathcal{K}$ are either zeros or positive. We will explain later why the covariance matrix must be positive semi-definite even in the case where eigen decomposition is used to calculate the coloring matrix. The covariance matrix $\mathcal{K}$, in fact, may *not* be positive semi-definite, i.e. $\mathcal{K}$ may have negative eigenvalues, as the case mentioned in Example 4.1 of Section IV-A.

To overcome this obstacle, similarly to (but not exactly as) the method in [13], we approximate the given covariance matrix by a matrix that can be decomposed into $\mathbf{K} = \mathbf{L}\mathbf{L}^H$. While the method in [13] does this by replacing all negative and zero eigenvalues by a small, positive real number, we only replace the negative ones by zeros. This is possible, because we base our decomposition on an eigen analysis instead of a Cholesky decomposition as in [13], which can only be carried out if all eigenvalues are positive. Our procedure is presented as follows.

Assuming that $\mathcal{K}$ is the desired covariance matrix, which is *not* positive semi-definite. Perform the *eigen decomposition* $\mathcal{K} = \mathbf{V}\mathbf{G}\mathbf{V}^H$, where $\mathbf{V}$ is the matrix of eigenvectors and $\mathbf{G}$ is a diagonal matrix of eigenvalues of the matrix $\mathcal{K}$. Let $\mathbf{G} = diag(\lambda_1, \ldots, \lambda_N)$. Calculate the approximate matrix $\mathbf{\Lambda} \triangleq diag(\hat{\lambda}_1, \ldots, \hat{\lambda}_N)$, where:

$$\hat{\lambda}_j = \begin{cases} \lambda_j & \text{if } \lambda_j \geq 0 \\ 0 & \text{if } \lambda_j < 0 \end{cases}$$

We now compare our approximation procedure to the approximation procedure mentioned in [13]. The authors in [13] used the following approximation:

$$\hat{\lambda}_j = \begin{cases} \lambda_j & \text{if } \lambda_j > 0 \\ \varepsilon & \text{if } \lambda_j \leq 0 \end{cases}$$

where ε is a small, positive real number.

Clearly, besides overcoming the disadvantage of Cholesky decomposition, our approximation procedure is *more precise* under realistic assumptions like finite precision arithmetic than the one mentioned in [13], since the matrix $\mathbf{\Lambda}$ in our algorithm approximates to the matrix $\mathbf{G}$ better than the one mentioned in [13]. Therefore, the desired covariance matrix $\mathcal{K}$ is well approximated by the positive semi-definite matrix $\mathbf{K} = \mathbf{V}\mathbf{\Lambda}\mathbf{V}^H$ from Frobenius point of view [13].

C. Determine the Coloring Matrix Using Eigen Decomposition

In most of the conventional methods, Cholesky decomposition was used to determine the coloring matrix. As analyzed earlier in Section II, Cholesky decomposition may not work for the covariance matrix which has eigenvalues being equal or close to zeros.

To overcome this disadvantage, we use eigen decomposition, instead of Cholesky decomposition, to calculate the coloring matrix. Comparison of the computational efforts between the two methods (eigen decomposition versus Cholesky decomposition) is mentioned later in this paper. The coloring matrix is calculated as follow:

At this stage, we have the forced positive semi-definite covariance matrix $\mathbf{K}$, which is equal to the desired covariance matrix $\mathcal{K}$ if $\mathcal{K}$ is positive semi-definite, or approximates to $\mathcal{K}$ otherwise. Further, as mentioned earlier, we have $\mathbf{K} = \mathbf{V}\mathbf{\Lambda}\mathbf{V}^H$, where $\mathbf{\Lambda} = diag(\hat{\lambda}_1, \ldots, \hat{\lambda}_N)$ is the matrix of eigenvalues of $\mathbf{K}$. Since $\mathbf{K}$ is a positive semi-definite matrix, it follows that $\{\hat{\lambda}_j\}_{j=1}^N$ are *real* and *non-negative*.

We now calculate a new matrix $\bar{\mathbf{\Lambda}}$ as:

$$\bar{\mathbf{\Lambda}} \;=\; \sqrt{\mathbf{\Lambda}} = diag\left(\sqrt{\hat{\lambda}_1}, \ldots, \sqrt{\hat{\lambda}_N}\right) \tag{11}$$

Clearly, $\bar{\mathbf{\Lambda}}$ is a *real*, *diagonal* matrix that results in:

$$\bar{\mathbf{\Lambda}}\bar{\mathbf{\Lambda}}^H \;=\; \bar{\mathbf{\Lambda}}\bar{\mathbf{\Lambda}} = \mathbf{\Lambda} \tag{12}$$

If we denote $\mathbf{L} \triangleq \mathbf{V}\bar{\mathbf{\Lambda}}$, then it follows that:

$$\mathbf{L}\mathbf{L}^H \;=\; (\mathbf{V}\bar{\mathbf{\Lambda}})(\mathbf{V}\bar{\mathbf{\Lambda}})^H = \mathbf{V}\bar{\mathbf{\Lambda}}\bar{\mathbf{\Lambda}}^H\mathbf{V}^H = \mathbf{V}\mathbf{\Lambda}\mathbf{V}^H = \mathbf{K} \tag{13}$$

It means that the coloring matrix $\mathbf{L}$ corresponding to the covariance matrix $\mathbf{K}$ can be computed *without* using Cholesky decomposition. Thereby, the shortcoming of the paper [13], which is related to round-off errors in Matlab caused by Cholesky decomposition and is pointed out in Section II, can be overcome.

We now explain why the covariance matrix must be positive semi-definite even when eigen decomposition is used to compute the coloring matrix. It is easy to realize that, if $\mathbf{K}$ is *not* positive semi-definite

covariance matrix, then $\bar{\mathbf{\Lambda}}$ calculated by (11) is a *complex* matrix. As a result, (12) and (13) are not satisfied.

D. Proposed Algorithm

In Section II, we have shown that the method proposed in [13] fails to generate Rayleigh fading envelopes corresponding to a desired covariance matrix in a real-time scenario where Doppler frequency shifts are considered. This is because the authors in [13] did not realize the variance-changing effect caused by Doppler filters.

To surmount this shortcoming, the two following *simple, but important* modifications must be carried out:

1) Unlike step 6 of the method in [13], where N independent, complex Gaussian random variables (with Rayleigh fading envelopes) are generated with *unit* variances, in our algorithm, this step is modified in order to be able to generate independent, complex Gaussian random variables with *arbitrary* variances σ_g^2. Correspondingly, step 7 of the method in [13] must also be modified. Besides being more generalized, the modification of our algorithm in steps 6 and 7 allows us to combine correctly the outputs of Doppler filters in the method proposed in [12] and our algorithm.
2) The variance-changing effect of Doppler filters must be considered. It means that, we have to calculate the variance of the outputs of Doppler filters, which may have an *arbitrary* value depending on the variance of the complex Gaussian random variables at the inputs of Doppler filters as well as the characteristics of those filters. The variance value of the outputs is then input into the step 6 which has been modified as mentioned above.

The modification 1 can be carried out in the algorithm generating Rayleigh fading envelopes in a *discrete-time* scenario (see the algorithm mentioned in this section). The modification 2 can be carried out in the algorithm generating Rayleigh fading envelopes in a real-time scenario *where Doppler frequency shifts are considered* (see the algorithm mentioned in Section V).

From the above observations, we propose here a generalized algorithm to generate N correlated Rayleigh envelopes in a *single time instant* as given below:

1) In a general case, the desired variances (powers) $\{{\sigma_g}_j^2\}_{j=1}^N$ of complex Gaussian random variables with Rayleigh envelopes must be known. Specially, if one wants to generate Rayleigh envelopes

corresponding to the desired variances (powers) $\{{\sigma_{r_j}}^2\}_{j=1}^N$, then $\{{\sigma_{g_j}}^2\}_{j=1}^N$ are calculated as follows[3]:

$$ {\sigma_{g_j}}^2 = \frac{{\sigma_{r_j}}^2}{(1-\frac{\pi}{4})} \quad \forall j = 1 \dots N \tag{14} $$

2) From the desired correlation properties of correlated complex Gaussian random variables with Rayleigh envelopes, determine the covariances $R_{xxk,j}$, $R_{yyk,j}$, $R_{xyk,j}$ and $R_{yxk,j}$, for k, $j = 1, \dots, N$ and $k \neq j$. In other words, in a general case, those covariances must be known.

   Specially, in the case where the powers of all random processes are *equal* and other conditions hold as mentioned in Section III-A and III-B, we can follow equations (3) and (4) in the case of time delay and frequency separation, such as in OFDM systems, or equations (5), (6) and (7) in the case of spatial separation like with multiple antennas in MIMO systems to calculate the covariances $R_{xxk,j}$, $R_{yyk,j}$, $R_{xyk,j}$ and $R_{yxk,j}$.

   The values $\{{\sigma_{g_j}}^2\}_{j=1}^N$, $R_{xxk,j}$, $R_{yyk,j}$, $R_{xyk,j}$ and $R_{yxk,j}$ (k, $j = 1, \dots, N$; $k \neq j$) are the input data of our proposed algorithm.

3) Create the $N \times N$-sized covariance matrix $\mathcal{K}$:

$$ \mathcal{K} \;=\; [\mu_{k,j}]_{N \times N} \tag{15} $$

   where

$$ \mu_{k,j} = \begin{cases} {\sigma_{g_j}}^2 & \text{if } k \equiv j \\ (R_{xxk,j} + R_{yyk,j}) - i(R_{xyk,j} - R_{yxk,j}) & \text{if } k \neq j \end{cases} \tag{16} $$

   The covariance matrix of complex Gaussian random variables is considered here, as opposed to the covariance matrix of Rayleigh fading envelopes like in the conventional methods.

4) Perform the eigen decomposition:

$$ \mathcal{K} \;=\; \mathbf{V}\mathbf{G}\mathbf{V}^H $$

   Denote $\mathbf{G} \triangleq diag(\lambda_1, \dots, \lambda_N)$. Then, calculate a new diagonal matrix:

$$ \mathbf{\Lambda} = diag(\hat{\lambda}_1, \dots, \hat{\lambda}_N) $$

   where

$$ \hat{\lambda}_j = \begin{cases} \lambda_j & \text{if } \lambda_j \geq 0 \\ 0 & \text{if } \lambda_j < 0 \end{cases} \qquad j = 1, \dots, N. $$

[3]Note that ${\sigma_{g_j}}^2$ is the variance of *complex* Gaussian random variables, rather than the variance per dimension (real or imaginary). Hence, there is no factor of 2 in the denominator.

Thereby, we have a diagonal matrix $\mathbf{\Lambda}$ with all elements in the main diagonal being *real* and definitely *non-negative*.

5) Determine a new matrix $\bar{\mathbf{\Lambda}} = \sqrt{\mathbf{\Lambda}}$ and calculate the coloring matrix $\mathbf{L}$ by setting $\mathbf{L} = \mathbf{V}\bar{\mathbf{\Lambda}}$.
6) Generate a column vector $\mathbb{W}$ of N *independent* complex Gaussian random samples with zero means and *arbitrary, equal* variances σ_g^2:

$$\mathbb{W} = (u_1, \ldots, u_N)^T$$

We can see that the modification 1 takes place in this step of our algorithm and proceeds in the next step.

7) Generate a column vector $\mathbb{Z}$ of N *correlated* complex Gaussian random samples as follows:

$$\mathbb{Z} \;=\; \frac{\mathbf{L}\mathbb{W}}{\sigma_g} \triangleq (z_1 \ldots, z_N)^T$$

As shown later in the next section, the elements $\{z_j\}_{j=1}^N$ are zero-mean, (*correlated*) complex Gaussian random variables with variances $\{{\sigma_g}_j^2\}_{j=1}^N$. The N moduli $\{r_j\}_{j=1}^N$ of the Gaussian samples in $\mathbb{Z}$ are the *desired* Rayleigh fading envelopes.

E. Statistical Properties of the Resultant Envelopes

In this section, we check the covariance matrix and the variances (powers) of the resultant correlated complex Gaussian random samples as well as the variances (powers) of the resultant Rayleigh fading envelopes.

It is easy to check that $E(\mathbb{W}\mathbb{W}^H) = \sigma_g^2\mathbf{I}_N$, and therefore:

$$E(\mathbb{Z}\mathbb{Z}^H) \;=\; E\left(\frac{\mathbf{L}\mathbb{W}\mathbb{W}^H\mathbf{L}^H}{\sigma_g^2}\right) = E(\mathbf{L}\mathbf{L}^H) = \mathbf{K}$$

It means that the generated Rayleigh envelopes are corresponding to the forced positive semi-definite covariance matrix $\mathbf{K}$, which is, in turn, *equal* to the desired covariance matrix $\mathcal{K}$ in case $\mathcal{K}$ is *positive semi-definite*, or *well approximates* to $\mathcal{K}$ otherwise. In other words, the desired covariance matrix $\mathcal{K}$ of complex Gaussian random variables (with Rayleigh fading envelopes) is achieved.

In addition, note that the variance of the j^{th} Gaussian random variable in $\mathbb{Z}$ is the j^{th} element on the main diagonal of $\mathbf{K}$. Because $\mathbf{K}$ approximates to $\mathcal{K}$, the elements on the main diagonal of $\mathbf{K}$ are thus equal (or close) to ${\sigma_g}_j^2$s (see Eq. (15) and (16)). As a result, the resultant complex Gaussian random variables $\{z_j\}_{j=1}^N$ in $\mathbb{Z}$ have zero means and variances (powers) $\{{\sigma_g}_j^2\}_{j=1}^N$.

It is known that the means and the variances of Rayleigh envelopes $\{r_j\}_{j=1}^N$ have the relation with the variances of the corresponding *complex* Gaussian random variables $\{z_j\}_{j=1}^N$ in $\mathbb{Z}$ as given below (see (5.51), (5.52) in [16] and (2.1-131) in [17]):

$$E\{r_j\} = \sigma_{g_j}\frac{\sqrt{\pi}}{2} = 0.8862\sigma_{g_j} \quad (17)$$

$$Var\{r_j\} = \sigma_{g_j}^2\big(1-\frac{\pi}{4}\big) = 0.2146\sigma_{g_j}^2 \quad (18)$$

From (14), (17) and (18), it is clear that:

$$E\{r_j\} = \sigma_{rj}\sqrt{\frac{\pi}{4-\pi}}$$

$$Var\{r_j\} = \sigma_{r_j}^2$$

Therefore, the *desired* variances (powers) $\{\sigma_{r_j}^2\}_{j=1}^N$ of Rayleigh envelopes are achieved.

V. Generation of Correlated Rayleigh Envelopes in a Real-Time Scenario

In Section IV-D, we have proposed the algorithm for generating N correlated Rayleigh fading envelopes in multipath, flat fading channels in a *single time instant*. We can repeat steps 6 and 7 of this algorithm to generate Rayleigh envelopes in the *continuous time interval*. It is noted that, the discrete-time samples of each Rayleigh fading process generated by this algorithm in *different* time instants are *independent* of each other.

It has been known that the discrete-time samples of each *realistic* Rayleigh fading process may have *autocorrelation* properties, which are the functions of the Doppler frequency corresponding to the motion of receivers as well as other factors such as the sampling frequency of transmitted signals. It is because the band-limited communication channels not only limit the bandwidth of transmitted signals, but also limit the bandwidth of fading. This filtering effect limits the rate of changes of fading in time domain, and consequently, results in the autocorrelation properties of fading. Therefore, the algorithm generating Rayleigh fading envelopes in *realistic* conditions must consider the autocorrelation properties of Rayleigh fading envelopes.

To simulate a multipath fading channel, Doppler filters are normally used [16]. The analysis of Doppler spectrum spread was first derived by Gans [18], based on Clarke's model [19]. Motivated by these works, Smith [20] developed a computer-assisted model generating an *individual* Rayleigh fading envelope in flat fading channels corresponding to a given *normalized autocorrelation* function. This model was then modified by Young [10], [12] to provide more accurate channel realization.

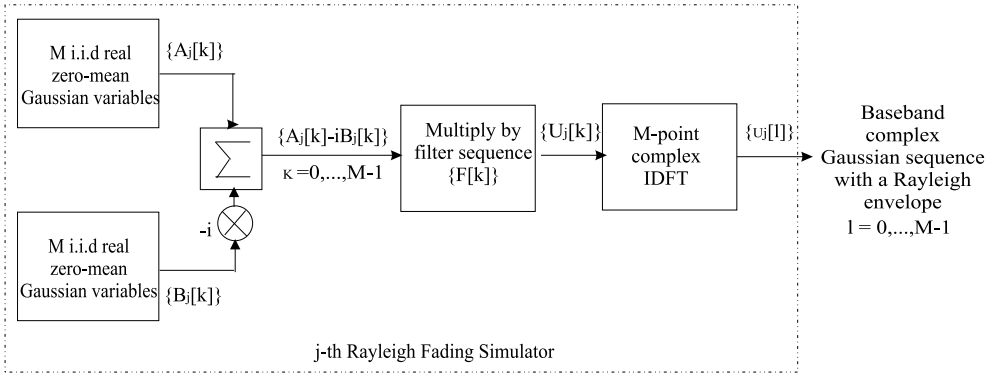

Fig. 2. Model of a Rayleigh generator for an individual Rayleigh envelope corresponding to a desired *normalized* autocorrelation function.

It should be emphasized that, in [10], [12], the models are aimed at generating an *individual* Rayleigh envelope corresponding to a certain normalized *autocorrelation* function of itself, rather than generating different Rayleigh envelopes corresponding to a desired covariance matrix (*autocorrelation* and *cross-correlation* properties between those envelopes).

Therefore, the model for generating N correlated Rayleigh fading envelopes in realistic fading channels (each individual envelope is corresponding to a desired normalized autocorrelation property) can be created by associating the model proposed in [12] with our algorithm mentioned in Section IV-D in such a way that, the resultant Rayleigh fading envelopes are corresponding to the desired covariance matrix.

This combination must overcome the main shortcoming of the method proposed in [13] as analyzed in Section II. In other words, the modification 2 mentioned in Section IV-D must be carried out. This is an easy task in our algorithm. The key for the success of this task is the modification in steps 6 and 7 of our algorithm (see Section IV-D), where the variances of N complex Gaussian random variables are *not fixed* as in [13], but can be *arbitrary* in our algorithm. Again, besides being more generalized, our modification in these steps allows the *accurate* combination of the method proposed in [12] and our algorithm, i.e. guaranteeing that the generated Rayleigh envelopes are exactly corresponding to the desired covariance matrix.

The model of a Rayleigh fading generator for generating an *individual* baseband Rayleigh fading envelope proposed in [10], [12] is shown in Fig. 2. This model generates a Rayleigh fading envelope using Inverse Discrete Fourier Transform (IDFT), based on *independent* zero-mean Gaussian random variables weighted by appropriate Doppler filter coefficients. The sequence $\{u_j[l]\}_{l=0}^{M-1}$ of the complex Gaussian random samples at the output of the j^{th} Rayleigh generator (Fig. 2) can be expressed as:

$$u_j[l] = \frac{1}{M} \sum_{k=0}^{M-1} U_j[k] e^{i\frac{2\pi kl}{M}}$$

where

M denotes the number of points with which the IDFT is carried out;

l is the discrete-time sample index ($l = 0, \ldots, M-1$);

$U_j[k]$=$F[k]A_j[k] - iF[k]B_j[k]$;

$\{F[k]\}$ are the Doppler filter coefficients.

For brevity, we omit the subscript j in the expressions, except when this subscript is necessary to emphasize. If we denote $u[l]$=$u_R[l] + iu_I[l]$, then it has been proved that, the *autocorrelation* property between the real parts $u_R[l]$ and $u_R[m]$ as well as that between the imaginary parts $u_I[l]$ and $u_I[m]$ at different discrete-time instants l and m is as given below (see Eq. (7) in [12]):

$$r_{RR}[l,m] = r_{II}[l,m] = r_{RR}[d] = r_{II}[d] = E\{u_R[l]u_R[m]\} = \frac{\sigma^2_{orig}}{M} Re\{g[d]\} \tag{19}$$

where $d \triangleq l - m$ is the sample lag, σ^2_{orig} is the variance of the *real*, independent zero-mean Gaussian random sequences $\{A[k]\}$ and $\{B[k]\}$ at the inputs of Doppler filters, and the sequence $\{g[d]\}$ is the IDFT of $\{F[k]^2\}$, i.e.:

$$g[d] = \frac{1}{M} \sum_{k=0}^{M-1} F[k]^2 e^{i\frac{2\pi kd}{M}} \tag{20}$$

Similarly, the correlation property between the real part $u_R[l]$ and the imaginary part $u_I[m]$ is calculated as (see Eq. (8) in [12]):

$$r_{RI}[d] = E\{u_R[l]u_I[m]\} = \frac{\sigma^2_{orig}}{M} Im\{g[d]\} \tag{21}$$

The mean value of the output sequence $\{u[l]\}$ has been proved to be zero (see Appendix A in [12]).

If d=0 and $\{F[k]\}$ are real, from (19), (20) and (21), we have:

$$\begin{aligned} r_{RR}[0] &= r_{II}[0] = E\{u_R[l]u_R[l]\} = \frac{\sigma^2_{orig}}{M^2} \sum_{k=0}^{M-1} F[k]^2 \\ r_{RI}[0] &= E\{u_R[l]u_I[l]\} = 0 \end{aligned}$$

Therefore, by definition, the variance of the sequence $\{u[l]\}$ at the output of the Rayleigh generator is:

$$\sigma_g^2 \triangleq E\{u[l]u[l]^*\} = 2E\{u_R[l]u_R[l]\} = \frac{2\sigma^2_{orig}}{M^2} \sum_{k=0}^{M-1} F[k]^2 \tag{22}$$

where * denotes the complex conjugate operation.

Let r_{nor} be:

$$r_{nor} = \frac{r_{RR}[d]}{\sigma_g^2} = \frac{r_{II}[d]}{\sigma_g^2} \tag{23}$$

i.e. r_{nor} be the autocorrelation function in (19) *normalized* by the variance σ_g^2 in (22). r_{nor} is called the *normalized autocorrelation* function.

To achieve a desired *normalized autocorrelation* function $r_{nor} = J_0(2\pi f_m d)$, where f_m is the maximum Doppler frequency F_m normalized by the sampling frequency F_s of the transmitted signals (i.e. $f_m = \frac{F_m}{F_s}$), the Doppler filter $\{F[k]\}$ is determined in Young's model [10], [12] as follows (see Eq. (21) in [12]):

$$F[k] = \begin{cases} 0 & k = 0 \\ \sqrt{\frac{1}{2\sqrt{1-\left(\frac{k}{Mf_m}\right)^2}}} & k = 1, \ldots, k_m - 1 \\ \sqrt{\frac{k_m}{2}\left[\frac{\pi}{2} - arctan\left(\frac{k_m - 1}{\sqrt{2k_m - 1}}\right)\right]} & k = k_m \\ 0 & k = k_m + 1, \ldots, M - k_m - 1 \\ \sqrt{\frac{k_m}{2}\left[\frac{\pi}{2} - arctan\left(\frac{k_m - 1}{\sqrt{2k_m - 1}}\right)\right]} & k = M - k_m \\ \sqrt{\frac{1}{2\sqrt{1-\left(\frac{M-k}{Mf_m}\right)^2}}} & k = M - k_m + 1, \ldots, M - 2, M - 1 \end{cases} \quad (24)$$

In (24), $k_m \triangleq \lfloor f_m M \rfloor$, where $\lfloor . \rfloor$ indicates the biggest rounded integer being less or equal to the argument.

It has been proved in [12] that the (real) filter coefficients in (24) will produce a complex Gaussian sequence with the *normalized autocorrelation* function $J_0(2\pi f_m d)$, and with the *expected independence* between the real and imaginary parts of Gaussian samples, i.e., the correlation property in (21) is zero. The zero-correlation property between the real and imaginary parts is necessary in order that the resultant envelopes are Rayleigh distributed.

Let us consider the variance σ_g^2 of the resultant complex Gaussian sequence at the output of Fig. 2. We consider an example where $M = 4096$, $f_m = 0.05$ and $\sigma_{orig}^2 = 1/2$ (σ_{orig}^2 is the variance per dimension). From (22) and (24), we have $\sigma_g^2 = 1.8965.10^{-5}$. Clearly, passing complex Gaussian random variables with unit variances through Doppler filters reduces significantly the variances of those variables. In general, the variances of the complex Gaussian random variables at the output of the Rayleigh simulator presented in Fig. 2 can be *arbitrary*, depending on M, σ_{orig}^2 and $\{F[k]\}$, i.e. depending on the variances of the Gaussian random variables at the inputs of Doppler filters as well as the characteristics of those filters (see Eq. (22) for more details).

We now return to the main shortcoming of the method proposed in [13], which is mentioned earlier in Section II. In Section VI of the paper [13], the authors generated Rayleigh envelopes corresponding to a desired covariance matrix in a *real-time scenario*, where Doppler frequency shifts were considered, by combining their proposed method with the method proposed in [12]. Specifically, the authors took the outputs of the method in [12] and *simply* input them into step 6 in their method.

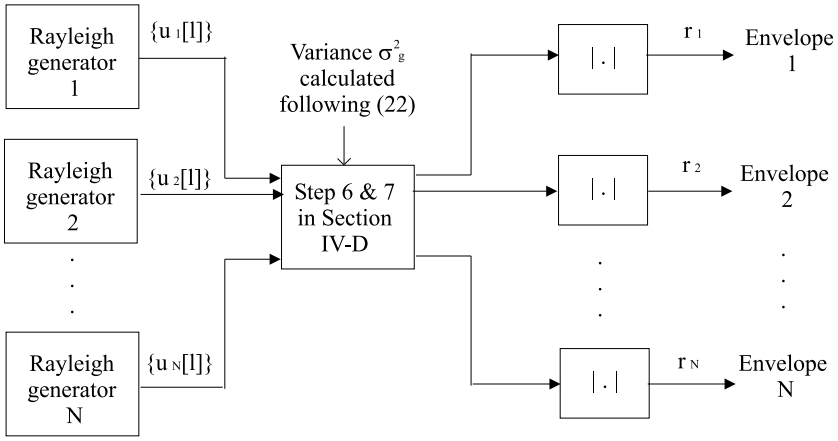

Fig. 3. Model for generating N Rayleigh envelopes corresponding to a desired *normalized* autocorrelation function in a real-time scenario.

However, the step 6 in the method in [13] was proposed for generating complex Gaussian random variables with a *fixed* (unit) variance. Meanwhile, as presented earlier, the variances of the complex Gaussian random variables at the output of the Rayleigh simulator may have *arbitrary* values, depending on the variances of the Gaussian random variables at the inputs of Doppler filters as well as the characteristics of those filters. Consequently, if the outputs of the method in [12] are simply input into the step 6 as mentioned in the algorithm in [13], the covariance matrix of the resultant correlated Gaussian random variables is *not* equal to the desired covariance matrix due to the variance-changing effect of Doppler filters being *not* considered. In other words, the method proposed in [13] *fails* to generate Rayleigh fading envelopes corresponding to a desired covariance matrix in a real-time scenario where Doppler frequency shifts are taken into account.

Our model for generating N correlated Rayleigh fading envelopes corresponding to a desired covariance matrix in a real-time scenario where Doppler frequency shifts are considered is presented in Fig. 3. In this model, N Rayleigh generators, each of which is presented in Fig. 2, are simultaneously used. To generate N *correlated* Rayleigh envelopes corresponding to a desired covariance matrix at *an observed discrete-time instant* l ($l = 0, \ldots, M-1$), similarly to the method in [13], we take the output $u_j[l]$ of the j^{th} Rayleigh simulator, for $j = 1, \ldots, N$, and input it as the element u_j into step 6 of our algorithm proposed in Section IV-D. However, as opposed to the method in [13], the variance σ_g^2 of complex Gaussian samples u_j in step 6 of our method is calculated following (22). This value is used as the input parameter for steps 6 and 7 of our algorithm (see Fig. 3). Thereby, the variance-changing effect caused by Doppler filters is taken into consideration in our algorithm, and consequently, our proposed algorithm overcomes the main shortcoming of the method in [13].

The algorithm for generating N correlated Rayleigh envelopes (when Doppler frequency shifts are considered) *at a discrete-time instant* l, for $l = 0, \ldots, M-1$, can be summarized as:

1) Perform the steps 1 to 5 mentioned in Section IV-D.
2) From the *desired autocorrelation* properties (19) and (23) of each of the complex Gaussian random sequences (with Rayleigh fading envelopes), determine the values M and σ^2_{orig}. These values can be arbitrarily selected, provided that they bring about the desired autocorrelation properties. The value of M is also the number of points with which IDFT is carried out.
3) For each Rayleigh generator presented in Fig. 2, generate M identically independently distributed (i.i.d.), *real*, zero-mean Gaussian random samples $\{A[k]\}$ with the variance σ^2_{orig} and, independently, generate M i.i.d., *real*, zero-mean Gaussian samples $\{B[k]\}$ with the distribution (0,σ^2_{orig}). From $\{A[k]\}$ and $\{B[k]\}$, generate M i.i.d complex Gaussian random variables $\{A[k]-iB[k]\}$. N Rayleigh generators are simultaneously used to generate N Rayleigh envelopes as presented in Fig. 3.
4) Multiply complex Gaussian samples $\{A[k]-iB[k]\}$, for $k = 1, \ldots, M$, with the corresponding filter coefficient $F[k]$ given in (24).
5) Perform M-point IDFT of the resultant samples.
6) Calculate the variance σ^2_g of the output $\{u[l]\}$ following (22). It is noted that σ^2_g is the same for N Rayleigh generators. We also emphasize that, by this calculation, the modification 2 mentioned in Section IV-D has been performed in this step.
7) Create a column vector $\mathbb{W} = (u_1, \ldots, u_N)^T$ of N i.i.d. complex Gaussian random samples with the distribution (0,σ^2_g) where the element u_j, for $j = 1, \ldots, N$, is the output $u_j[l]$ of the j^{th} Rayleigh generator and σ^2_g has been calculated in step 6.
8) Continue the step 7 mentioned in Section IV-D. The N envelopes of elements in the column vector $\mathbb{Z}$ are the desired Rayleigh envelopes *at the considered time instant* l.

Steps 7 and 8 are repeated for different time instants l ($l = 0, \ldots, M-1$), and therefore, the algorithm can be used for a real-time scenario.

VI. Simulation Results

In this section, first, we simulate N=3 *frequency-correlated* Rayleigh fading envelopes corresponding to the complex Gaussian random variables with equal powers $\sigma^2_{g_j} = 1$ ($j = 1, \ldots, 3$) in the flat fading channels. Parameters considered here include $M = 2^{14}$ (the number of IDFT points), $\sigma^2_{orig} = 1/2$ (variances per dimension in Young's model), $F_s = 8$ KHz, $F_m = 50$ Hz (corresponding to a carrier frequency 900

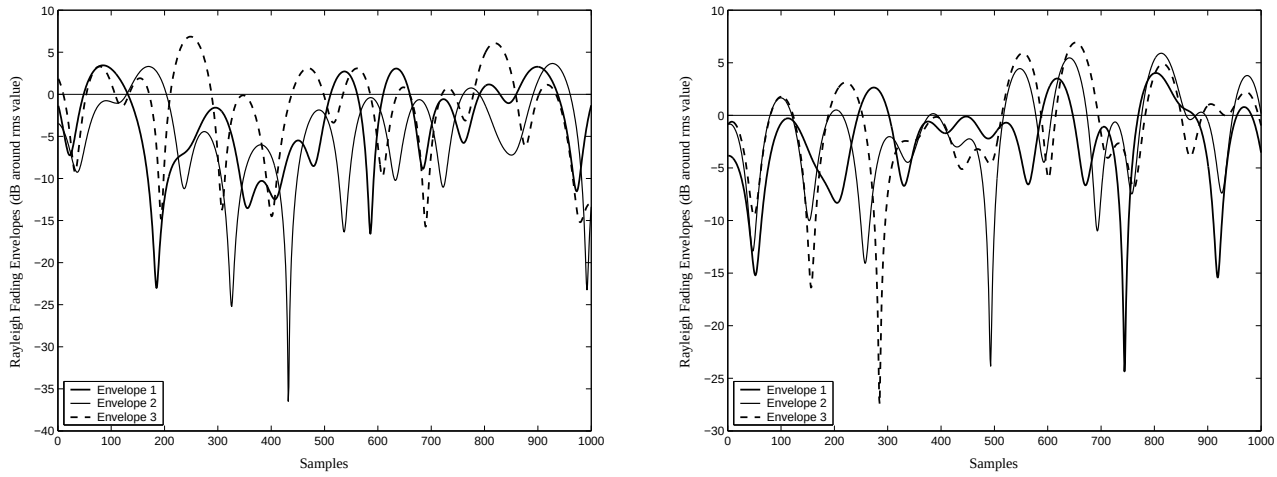

(a) Spectral correlation, GSM specifications

(b) Spatial correlation, GSM specifications

Fig. 4. Examples of three equal power correlated Rayleigh fading envelopes with GSM specifications.

MHz and a mobile speed $v = 60$ km/hr). Frequency separation between two adjacent carrier frequencies considered here is $\Delta f = 200$ kHz (e.g in GSM 900) and we assume that $f_1 > f_2 > f_3$. Also, we consider the rms delay spread $\sigma_\tau = 1\mu s$ and time delays between three envelopes are $\tau_{1,2} = 1ms$, $\tau_{2,3} = 3ms$, $\tau_{1,3} = 4ms$.

From (3), (4), (15) and (16), we have the *desired* covariance matrix $\mathcal{K}$ as given below:

$$\mathcal{K} = \begin{bmatrix} 1 & 0.3782 + 0.4753i & 0.0878 + 0.2207i \\ 0.3782 - 0.4753i & 1 & 0.3063 + 0.3849i \\ 0.0878 - 0.2207i & 0.3063 - 0.3849i & 1 \end{bmatrix} \tag{25}$$

It is easy to check that $\mathcal{K}$ in (25) is positive definite. Using the proposed algorithm in Section V, we have the simulation result presented in Fig. 4(a).

Next, we simulate N=3 *spatially-correlated* Rayleigh fading envelopes. We consider an antenna array comprising three transmitter antennas, which are equally separated by a distance D. Assume that $\frac{D}{\lambda} = 1$, i.e., $D = 33.3$ cm for GSM 900. Additionally, we assume that $\Delta = \pi/18$ rad (or $\Delta = 10^\circ$) and $\Phi = 0$ rad. The parameters M, $\sigma_{g_j}^2$, σ_{orig}^2, F_s and F_m are the same as in the previous case. From (5), (6), (7), (15) and (16), we have the following *desired* covariance matrix:

$$\mathcal{K} = \begin{bmatrix} 1 & 0.8123 & 0.3730 \\ 0.8123 & 1 & 0.8123 \\ 0.3730 & 0.8123 & 1 \end{bmatrix} \tag{26}$$

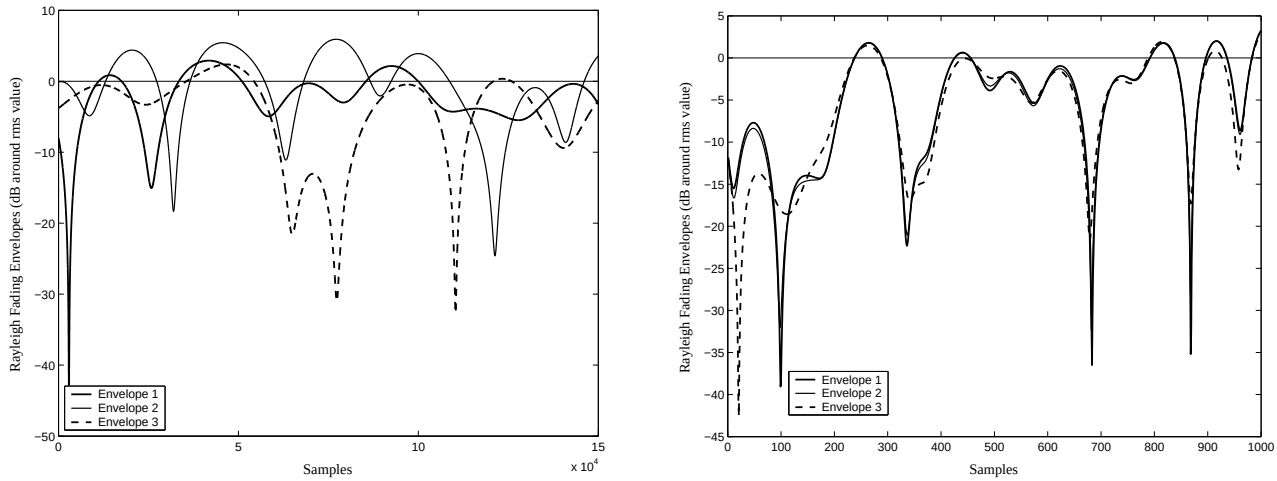

(a) Spectral correlation, OFDM specifications

(b) Spatial correlation, $\mathcal{K}$ is not positive semi-definite

Fig. 5. Examples of three equal power correlated Rayleigh fading envelopes with IEEE 802.11a (OFDM) specifications, and with a not positive semi-definite covariance matrix.

Since $\Phi = 0$ rad, the covariances $R_{xy_{k,j}}$ and $R_{yx_{k,j}}$ between the real and imaginary components of any pair of the complex Gaussian random processes (with Rayleigh fading envelopes) are zeros, and consequently, $\mathcal{K}$ is a *real* matrix. Readers may refer to (6) and (7) for more details. It is easy to realize that $\mathcal{K}$ in (26) is positive definite. The simulation result is presented in Fig. 4(b).

In Fig. 5(a), we simulate N=3 *frequency-correlated* Rayleigh envelopes based on IEEE 802.11a (OFDM) specifications [21]. In particular, the parameters considered here include $M = 2^{20}$, $\sigma_{g_j}^2 = 1$ ($j = 1, \ldots, 3$), $\sigma_{orig}^2 = 1/2$, $F_s = 20$ MHz, $F_m = 555.56$ Hz (corresponding to a carrier frequency 5 GHz and a mobile speed $v = 120$ km/hr), $\Delta f = 312.5$ kHz, $\sigma_\tau = 0.1\mu s$, $\tau_{1,2} = \tau_{2,3} = 1ms$, and $\tau_{1,3} = 2ms$. In Fig. 5(b), we simulate the case where the covariance matrix is not positive semi-definite as mentioned earlier in Example 4.1 of Section IV-A. From Fig. 5(b), we can realize that the three Rayleigh envelopes are highly correlated as we expect (see Eq. (10)).

In Fig. 6, we plot the histograms of the resultant Rayleigh fading envelopes produced by our algorithm in the four aforementioned examples. Without loss of generality, we plot the histograms for one of three Rayleigh fading envelopes, such as the first Rayleigh fading envelope. To compare the accuracy of our algorithm, we also plot the *theoretical* probability density function (PDF) of a typical Rayleigh fading envelope by solid curves. In this figure, the parameter $\sigma_{g_j}^2$ of the PDF is the variance of the *complex* Gaussian random process corresponding to the considered typical Rayleigh fading envelope. It can be observed from Fig. 6 that, the resultant envelopes produced by our algorithm in the four examples follow

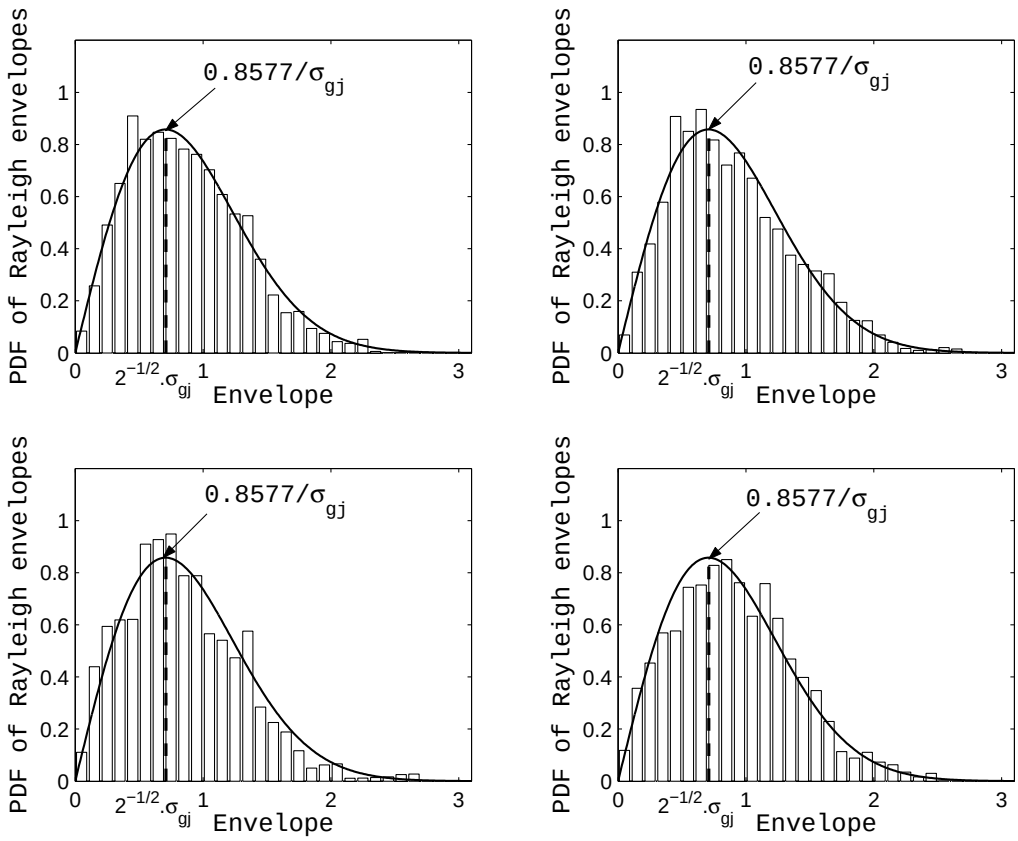

Fig. 6. Histograms of Rayleigh fading envelopes produced by the proposed algorithm in the four examples along with a Rayleigh PDF where $\sigma_{g_j}^2 = 1$.

accurately the theoretical PDF of the typical Rayleigh fading envelope.

Finally, in Fig. 7, we compare the computational efforts between our algorithm and the one mentioned in [13], by comparing the average computational time required for both algorithms to simulate N = 2, 4, 8, 16, 32, 64 or 128 Rayleigh envelopes in a real-time scenario over 10000 trials. It can be realized from Fig. 7 that, for $N = 64$ and $N = 128$, our algorithm is slightly more complex, while it is almost as computationally efficient as the method in [13] for a smaller N.

VII. Conclusions

In this paper, we have derived a more generalized algorithm to generate correlated Rayleigh fading envelopes. Using the presented algorithm, one can generate an arbitrary number N of *either* Rayleigh envelopes with any desired power $\sigma_{r_j}^2$, $j = 1, \ldots, N$, *or* those envelopes corresponding to any desired power $\sigma_{g_j}^2$ of Gaussian random variables. This algorithm also facilitates to generate *equal* as well as *unequal* power Rayleigh envelopes. It is applicable to both scenarios of *spatial correlation* and *spectral correlation* between the random processes. The coloring matrix is determined by a positive

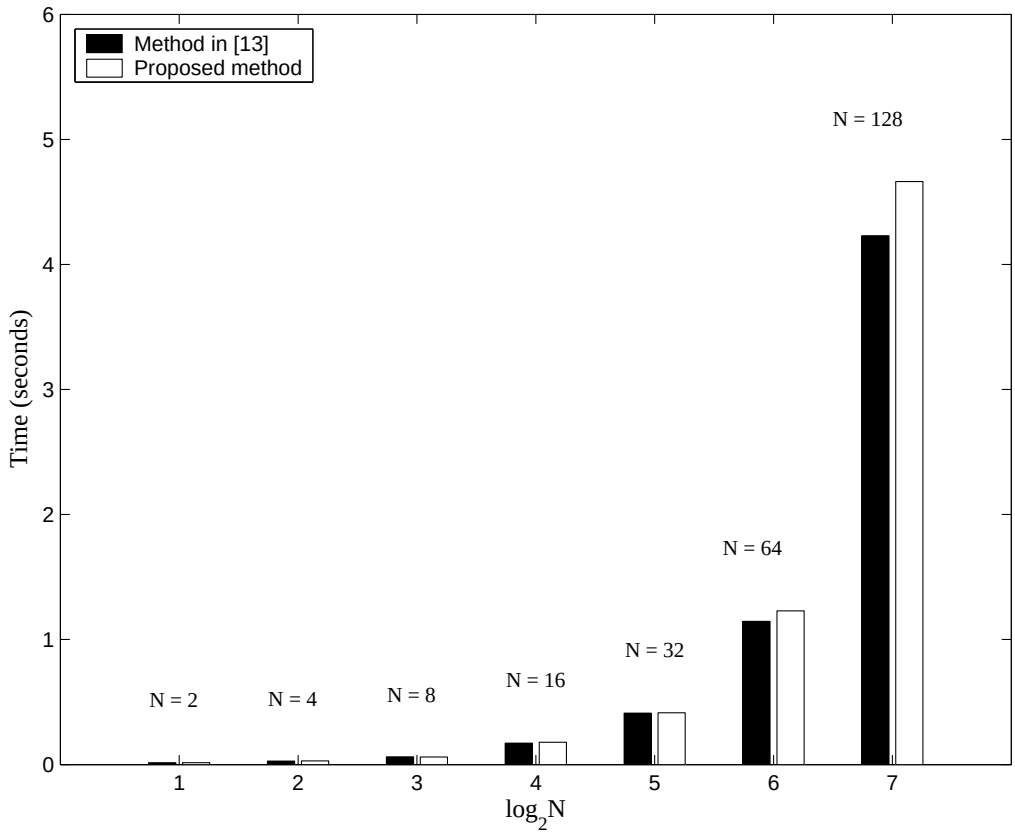

Fig. 7. Computational effort comparison between the method in [13] and the proposed algorithm.

semi-definiteness forcing procedure and an eigen decomposition procedure without using Cholesky decomposition. Consequently, the restriction on the positive definiteness of the covariance matrix is relaxed and the algorithm works well without being impeded by the roundoff errors of Matlab. The proposed algorithm can be used to generate Rayleigh envelopes corresponding to any desired covariance matrix, no matter whether or not it is positive definite. In comparison with the conventional methods, besides being *more generalized*, our proposed algorithm (with or without Doppler spectrum spread) is *more precise*, while overcoming all shortcomings of the conventional methods.

ACKNOWLEDGMENT

The authors would like to thank the reviewers for the very helpful comments.

REFERENCES

[1] D. Verdin and T. C. Tozer, “Generating a fading process for the simulation of land-mobile radio communications,” *Electronics Lett.*, vol. 29, no. 23, pp. 2011–2012, Nov. 1993.

[2] J. Salz and J. H. Winters, “Effect of fading correlation on adaptive arrays in digital mobile radio,” *IEEE Trans. Veh. Technol.*, vol. 43, no. 4, pp. 1049–1057, Nov. 1994.

[3] A. Hansson and T. Aulin, "Generation of N correlated Rayleigh fading processes for the simulation of space-time-selective radio channels," *Proc. European Wireless '99 / 4th ITG Conference on Mobile Communications*, pp. 269 – 272, Oct. 1999.

[4] N. C. Beaulieu and M. L. Merani, "Efficient simulation of correlated diversity channels," *Proc. IEEE Conference on Wireless Communications and Networking WCNC 2000*, vol. 1, pp. 207–210, Sept. 2000.

[5] C. A. G. D. de Leon, M. C. Bean, and J. S. Garcia, "On the generation of correlated Rayleigh envelopes for representing the variant behavior of the indoor radio propagation channel," *Proc. 15th IEEE Int. Symp. Personal, Indoor and Mobile Radio Commun. PIMRC 2004*, vol. 4, pp. 2757 – 2761, Sept. 2004.

[6] C. A. G. D. de Leon, M. C. Bean, and J. S. Garcia, "Generation of correlated Rayleigh-fading envelopes for simulating the variant behavior of indoor radio propagation channels," *Proc. 60th IEEE Veh. Technol. Conf. VTC 2004 - Fall*, vol. 6, pp. 4245 – 4249, Sept. 2004.

[7] R. B. Ertel and J. H. Reed, "Generation of two equal power correlated Rayleigh fading envelopes," *IEEE Commun. Lett.*, vol. 2, no. 10, pp. 276–278, Oct. 1998.

[8] N. C. Beaulieu, "Generation of correlated Rayleigh fading envelopes," *IEEE Commun. Lett.*, vol. 3, no. 6, pp. 172–174, June 1999.

[9] B. Natarajan, C. R. Nassar, and V. Chandrasekhar, "Generation of correlated Rayleigh fading envelopes for spread spectrum applications," *IEEE Commun. Lett.*, vol. 4, no. 1, pp. 9–11, Jan. 2000.

[10] D. J. Young and N. C. Beaulieu, "On the generation of correlated Rayleigh random variates by inverse discrete Fourier transform," *Proc. 5th IEEE International Conference on Universal Personal Communications ICUPC*, vol. 1, pp. 231–253, Oct. 1996.

[11] D. J. Young and N. C. Beaulieu, "A quantitative evaluation of generation methods for correlated Rayleigh random variates," *Proc. IEEE Global Telecommunications Conference GLOBECOM 98*, vol. 6, pp. 3332–3337, Nov. 1998.

[12] D. J. Young and N. C. Beaulieu, "The generation of correlated Rayleigh random variates by inverse discrete Fourier transform," *IEEE Trans. Commun.*, vol. 48, no. 7, pp. 1114–1127, July 2000.

[13] S. Sorooshyari and D. G. Daut, "Generation of correlated Rayleigh fading envelopes for accurate performance analysis of diversity systems," *Proc. 14th IEEE Int. Symp. Personal, Indoor and Mobile Radio Commun. PIMRC 2003*, vol. 2, pp. 1800–1804, Sept. 2003.

[14] H. Adeli and R. Soegiarso, *High-performance computing in structural engineering*, Boca CRC Press, Boca Raton, 1999.

[15] W. C. Jakes, *Microwave mobile communications*, John Wiley & Sons, New York, 1974.

[16] T. S. Rappaport, *Wireless communication: principles and practice*, Prentice Hall PTR, Upper Saddle River, N.J.; London, second edition, 2002.

[17] J. G. Proakis, *Digital communications*, McGraw-Hill, Boston, fourth edition, 2001.

[18] M. J. Gans, "A power spectral theory of propagation in the mobile radio environment," *IEEE. Trans. Veh. Technol.*, vol. VT-21, pp. 27–38, Feb. 1972.

[19] R. H. Clarke, "A statistical theory of mobile-radio reception," *Bell system technical journal*, vol. 47, pp. 957–1000, July 1968.

[20] J. I. Smith, "A computer generated multipath fading simulation for mobile radio," *IEEE Trans. Veh. Technol.*, vol. VT-24, no. 3, pp. 39–40, Aug. 1975.

[21] IEEE Standards Association, "Part 11: Wireless LAN medium access control (MAC) and physical layer (PHY) specifications - High-speed physical layer in the 5 GHz band," *IEEE Standards Association [Online]. Available: http://standards.ieee.org/getieee802/download/802.11a-1999.pdf [Accessed: 12 Apr., 2005]*, 1999.